2011 American Control Conference
on O'Farrell Street, San Francisco, CA, USA
June 29 - July 01, 2011

Frequency identification of nonparametric Hammerstein systems with backlash nonlinearity

A. Brouri, F. Giri*, Y. Rochdi, F.Z. Chaoui

Abstract— **We are considering the problem of identifying continuous-time Hammerstein systems that contain backlash nonlinearities. Both the linear and nonlinear parts are nonparametric and of unknown structure. In particular, the backlash nonlinearity borders are of arbitrary-shape and so may be nonsmooth and noninvertible. A two-stage frequency identification method is developed to get a set of points of the nonlinearity borders and estimates of the linear subsystem frequency gain at a number of frequencies. The method involves easily generated excitation signals and simple Fourier series decomposition based algorithms. All estimators are shown to be consistent.**

I. Introduction

The problem of identifying Hammerstein continuous-time systems is addressed in presence of memory input nonlinearities of backlash type (Fig 1). The memory nature of $F[.]$ implies that the backlash output, at a given time t, is not uniquely determined by the input $v(t)$ at the same time (Figs 2 and 3), furthermore, the internal signal is non measureable. In view of these difficulties, it is not surprising that few solutions are available that deal with Hammerstein system identification in presence of memory elements. Furthermore, most existing solutions focused on backlash bordered by straight lines, [1-3]. General nonparametric backlash elements, flanked by arbitrary-shape borders, have recently been considered in the discrete-time, together with parametric linear subsystems [4]. There, the identification problem was dealt with in two stages using periodic impulse inputs and least squares estimators. In each stage, a simultaneous estimation is performed of the linear subsystem parameters and a set of points of one border of the nonlinearity. In the present paper, the focus is made on the case where both the backlash nonlinearity and the linear subsystem are nonparametric. Unlike [4], the identification problem is dealt with in the continuous-time context, using a frequency approach involving periodic piecewise constant signal and Fourier series expansions. Here, the identification of the backlash nonlinearity is totally decoupled from the identification of the linear subsystem; each part being identified in a separate stage. The involved piecewise constant signals are quite simpler to generate than those used in [4]. Finally, the presently considered class of backlash nonlinearities is as general as in [4]. Accordingly, the nonparametric nonlinearity borders are allowed to be nonsmooth and noninvertible. Moreover, the borders may cross each other making possible to apply the proposed identification method to Hammerstein systems with memoryless (static) nonlinearities. In effect, a memoryless nonlinear operator can be seen as a backlash operator with superposed borders.

The paper is organized as follows: The identification problem is formally described in Section 2. The nonlinearity borders identification is dealt with in Section 3 and the linear subsystem identification is coped with in Section 4.

All authors are with the GREYC Lab, University of Caen, France
*Corresponding author (e-mail: fouad.giri@unicaen.fr).

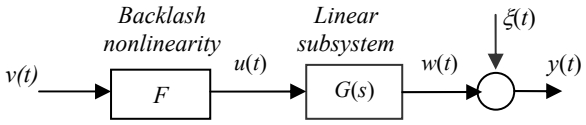

Fig. 1. Hammerstein System Model

II. Identification Problem Statement

We are interested in systems that can be described by the Hammerstein model (Fig. 1):

$$y(t) = w(t) + \xi(t), \quad t \in [0 + \infty) \tag{1}$$

$$w = G(s)u \quad \text{and} \quad u = F[v] \tag{2}$$

where $G(s)$ represents the linear subsystem transfer function, $F[.]$ the nonlinear operator and ξ a measurement noise. As the signals (u, w, ξ) are not accessible to measurements, system identification must only relay on the external signals v and y. The signal ξ is supposed to be a zero-mean ergodic white noise. The transfer function $G(s)$ has no known structure but it is asymptotically stable and with nonzero static gain (i.e. $G(0) \neq 0$). System stability is coherent with open-loop system identification. The fact that $G(0) \neq 0$ implies that, without reducing generality, one can assume $G(0) = 1$. Indeed, if the couple (F, G) is representative of the system, then so is any triplet of the form $(kF[.], G(s)/k)$, whatever $k \neq 0$. Finally, note that the nonzero static-gain requirement is satisfied by most real lifesystems. It is only not satisfied by derivative systems. When these are involved the proposed identification method can still be applied using ad-hoc adaptations.

The nonlinear element $F[.]$ is a backlash operator characterized by its ascendant and descendant lateral

borders, $(v, f_a(v))$ and $(v, f_d(v))$ (Fig.2). These borders assume no particular structure unlike in [1-3]. The backlash element operates as follows: suppose the nonlinearity working point, i.e. $(v(t), u(t))$, is moving along one border (either $f_a(.)$ or $f_d(.)$) and, at some instant t_0, the input v changes its variation sense i.e. $\lim_{\substack{t\to t_0 \\ t>t_0}} \operatorname{sgn}(\dot{v}(t)) \neq \lim_{\substack{t\to t_0 \\ t<t_0}} \operatorname{sgn}(\dot{v}(t))$. Then, the working point starts leaving the current border, moving horizontally towards the opposite border. If the input rate $\dot{v}(t)$ keeps the same sign, as $\lim_{\substack{t\to t_0 \\ t>t_0}} (\dot{v}(t))$, for a long time then, the working point will actually gets to the opposite border. Accordingly, if the input signal $v(t)$ spans monotonically in both senses a sufficiently wide working interval $[v_m \;\; v_M]$ then, the working point will span the backlash characteristic between the vertical lines $v = v_m$ and $v = v_M$, passing from one border to the other along two connecting horizontal paths, describing thus a closed backlash cycle. The system description is completed by the following remark.

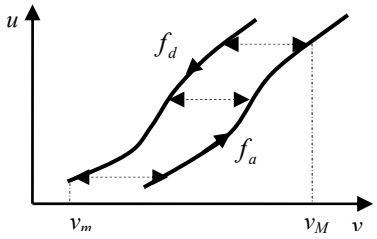

Fig. 2. Nonparametric backlash

Remark 1.

a) In case the working $[v_m \;\; v_M]$ interval is not sufficiently large, the resulting steady-state internal signal $u(t)$ will be constant i.e. the backlash working point will move along a horizontal segment. Then, the system output $y(t)$ becomes constant (up to noise) after a short transient period. This observation can be based upon in practice to discard non-suitable choices of $[v_m \;\; v_M]$.

b) The backlash bordering functions $f_a(.)$ or $f_d(.)$ are only supposed to be well defined and bounded within the considered working interval. Except for this assumption, $f_a(.)$ or $f_d(.)$ are arbitrary shape. In particular, they are allowed to be noninvertible and discontinuous, making possible to account for rely-type nonlinearities. Moreover, the borders are also allowed to cross each other (Fig. 3) making possible to account for memoryless (static) nonlinearities. Actually, memoryless nonlinearities can be seen as memory nonlinearities with superposed (ascendant and descendant) borders. This is a quite feature of the present study because any identification method that is supposed to work well for (Hammerstein systems with) backlash nonlinearities must be able to work equally well in the simpler case of memoryless (static) nonlinearities ('*he who can do more must be able to do less*').

c) It is worthy to emphasize that backlash nonlinearities with non-straight bordering lines are representative of many real-life control actuators e.g. industrial control valves. They may also arise as a consequence of combinations of simpler operators (Fig. 4).

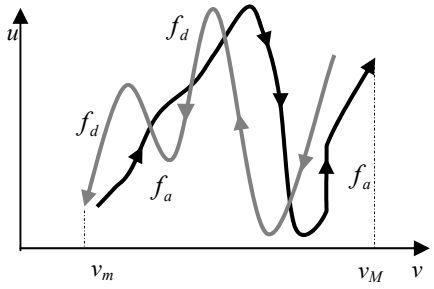

Fig 3. General shape backlash

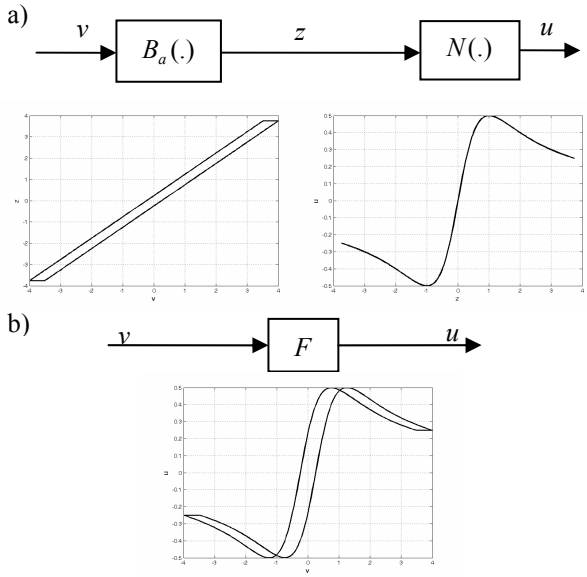

Fig. 4. a) series combination of a static nonlinearity and a backlash operator with straight-line borders. b: equivalent backlash operator with non-straight bordering lines.

d) Compared to [4], the present study deals with continuous-time fully nonparametric Hammerstein systems, while discontinuous parametric linear subsystems were considered in the above reference. Another major difference between the present study and [4] is that the considered identification methods are quite different. In [4] all parameters of the linear subsystems as well as (a set of points of one border of) the nonlinearity are identified simultaneously, using impulse sequences and least squares estimators; the other border is determined in a second step. In the present method, the linear and nonlinear parts are

identified sequentially, in two distinguished steps, using piecewise constant signals and Fourier series decomposition.

III. Backlash Nonlinearity Identification

In this section, we seek the estimation of a set of points on each border of the backlash nonlinearity. The number n of points is arbitrary but their abscissas must belong to the working interval $[v_m \;\; v_M]$. Let $V_1 = v_m < V_2 < \cdots < V_n = v_M$ be the selected abscissas. To determine the points $(V_i, f_a(V_i))$, one has first to make sure that the current working point, say $(v(t_0), u(t_0))$ is on the ascendant border. Then, letting $v(t) = V_i \quad (t \geq t_0)$, for some $V_i > v(t_0)$, ensures that the backlash working point $(v(t), u(t)) = (V_i, U_i)$ is still on the ascendant border i.e. $U_i = f_a(V_i)$. As the linear subsystem is asymptotically stable with unit static gain, it follows that the steady-state undisturbed output $w(t)$ is constant i.e. $w(t) \underset{t\to\infty}{\to} W_i$ with $W_i = G(0)U_i = f_a(V_i)$ (using the fact that $G(0) = 1$). Finally, notice that the steady state undisturbed output W_i can simply be estimated using the fact that $y(t) = w(t) + \xi(t)$ and $\xi(t)$ is zero-mean. Specifically, W_i can be recovered by averaging $y(t)$ on a sufficiently large interval. Hence, a number of points of the ascendant border (as well as points of one horizontal segment relating both borders) can thus be accurately estimated by repeating the above experiment successively for $V_1 \ldots V_n$. A symmetrical procedure could similarly be described to determine a number of points on the descendant border. These ideas are formalized in the three-stage identification procedure of Table 1, where T_r is theoretically any positive real number. Practically, it is convenient to let T_r be comparable to the system rise time i.e. the time that is necessary for a system step response to reach 90% of its final value. Then, as the system is asymptotically stable, its step undisturbed response settles down (i.e. gets very close to final value) after a transient period of nearly $3T_r$.

Also, in Table 1, $\mathcal{P}_a$ and $\mathcal{P}_d$ designate, respectively, the ascendant and descendant paths defined as follows (see Fig. 5):

- $\mathcal{P}_a$ is constituted of: (i) the horizontal segment relating point ① of coordinates $(v_m, f_d(v_m))$ to point ② on the ascendant border; (ii) the portion of this border between point ② and point ③ of coordinates $(v_M, f_a(v_M))$.
- $\mathcal{P}_d$ is constituted of: (i) the horizontal segment relating point ③ to point ④ on the descendant border; (ii) the portion of this border between point ④ and point ①.

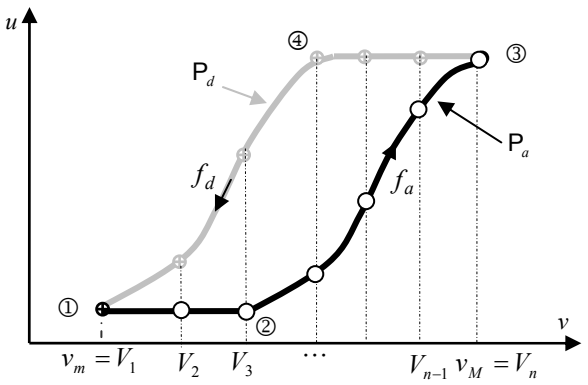

Fig. 5. Limit cycle described by the backlash working point (v,u), when the signal (4a-b) is applied. The circles represent the positions occupied by (v,u) during the time-interval $[0 \; nNT_r]$ and the crosses those occupied during $[nNT_r \;\; (2n-1)NT_r]$. The figure also shows the ascendant path $\mathcal{P}_a$ and descendant path $\mathcal{P}_d$.

Table 1. Nonparametric Backlash Border Identification (NBBI)

1. Initialization experiment

Apply the following step signal:

$$v(t) = \begin{cases} v_M & for \quad 0 \leq t < T_0 \\ v_m & for \quad T_0 \leq t < 2T_0 \end{cases} \tag{3}$$

where T_0 is an arbitrary small real such that $T_0 > 0$

2. Data acquisition

Choose an integer $N >> 1$.

Apply the piecewise signal represented by Fig. 6a, analytically defined as follows, for all $t \in [i\,NT_r \;\; (i+1)NT_r]$, $i = 0,\ldots,2n-3$:

$$v(t) = V_{i+1} \quad \text{for} \quad 0 \leq i \leq n-1 \tag{4a}$$

and

$$v(t) = V_{i+1} \;\; \text{with} \;\; V_{i+1} \overset{def}{=} V_{2n-i-1} \;\; \text{for} \;\; n \leq i \leq 2n-3$$
$$\text{and} \;\; V_{n+i} = V_{n-i} \;\; \text{for} \;\; (i = 1 \ldots n-1) \tag{4b}$$

Record the resulting output $y(t)$, $t \in [0 \;\; (2n-1)NT_r]$.

3. Border points estimation

Compute the (undisturbed output) mean value on each interval $[i\,NT_r \;\; (i+1)NT_r]$, $i = 0,\ldots,2n-3$:

$$\hat{W}_{i+1}(N) = \frac{1}{NT_r} \int_{iNT_r}^{(i+1)NT_r} y(t) \tag{5}$$

Then, the set of couples $\left(V_{i+1}, \hat{W}_{i+1}(N)\right)$, $i = 0,\ldots,n-1$, are estimates of n points all belonging to the ascendant path $\mathcal{P}_a$ and the couples $\left(V_{i+1}, \hat{W}_{i+1}(N)\right)$ with $V_{i+1} \overset{def}{=} V_{2n-i-1}$ for $i = n-1, n-2, \ldots 2n-3$, and $\left(V_1, \hat{W}_1(N)\right)$, are estimates of n points all located on the descendent path $\mathcal{P}_d$ (Fig. 5).

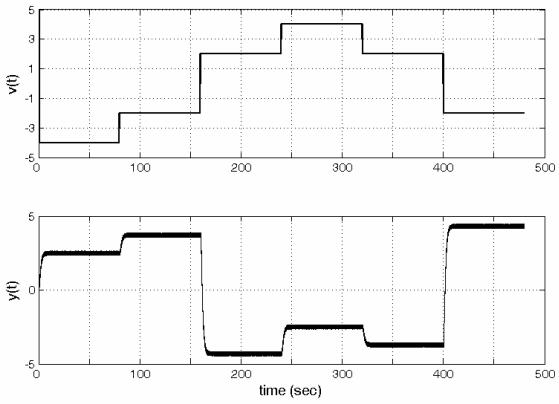

Fig.6. Above: Input signal (4a) applied in Stage 2 of the NBBI procedure with $n=4$. Below: Shape of the resulting disturbed output signal obtained with $G(s)=\dfrac{(s-10)}{(s+1)^2}$.

Before analyzing the NBBI procedure (Table 1), let us first comment on the involved experiments. The initialization experiment (Part 1), is just resorted to make sure that, afterward, the backlash working point (v,u) occupies position ① whose coordinates are $(v_m, f_d(v_m))$. Then, the input signal (4a) will enforce the working point to describe (a number of points of) the complete backlash cycle ① $\rightarrow$②$\rightarrow$③$\rightarrow$④$\rightarrow$①. More specifically, the working point moves on the ascendant path $\mathcal{P}_a$ for $t \in [0\ nNT_r]$ occupying there n positions (represented by circles in Fig. 5). For $t \in [nNT_r\ (2n-1)NT_r]$, the working point moves on the descendant path $\mathcal{P}_d$ occupying there $n-2$ positions (indicated by crosses in Fig. 5); Note that the particular points corresponding to $v(t)=v_m$ and $v(t)=v_M$ belong to both paths P_a and P_d. Note also that the last position, achieved on the time interval $t \in [(2n-3)\,NT_r\ (2n-2)NT_r]$ with $v(t)=V_2$. That is, the number of different positions occupied by the working point is in fact $2n-2$. Finally, note that each input value is kept on during $N\,T_r$ seconds to make sure that the output signal settles down within each interval of the form $[i\,NT_r\ (i+1)NT_r]$ (Fig. 6b).

Proposition 1. The points of coordinates $\left(V_{i+1}, \hat{W}_{i+1}(N)\right)$, $i=0\ldots n-1$, obtained in the NBBI procedure, with the data collected on the time interval $[0\ nNT_r]$, converge (in probability) to the ascendant path $\mathcal{P}_a$ as $N \rightarrow \infty$. Similarly, the points $\left(V_{i+1}, \hat{W}_{i+1}(N)\right)$, with $V_{i+1} \overset{def}{=} V_{2n-i-1}$ for $i=n,\ldots,2n-3$, obtained with the data collected on the interval $[nNT_r\ (2n-2)NT_r]$, converge to the descendent path $\mathcal{P}_d$ as $N \rightarrow \infty$ □

Proof. It has already been noticed that, after the initialization experiment (step 1 of the NBBI procedure), the backlash working point (v,u) occupies position ① with coordinates $(v_m, f_d(v_m))$. Then, it follows from (4a) that, for $t \in [0\ nNT_r]$, the working point $(v(t),u(t))$ moves on the ascendant path $\mathcal{P}_a$ occupying there n positions belonging to the set $\{(V_1, f_d(v_m)),\ (V_{i+1}, f_a(V_{i+1}); i=1,\ldots,n-1\}$, i.e. one has:

$$v(t)=V_1 \text{ and } u(t)=f_d(v_m),\ \forall t \in [0\ NT_r] \tag{6a}$$

and for any given $i=1,\ldots,n-1$

$$v(t)=V_{i+1} \text{ and } u(t)=f_a(V_{i+1}),\ \forall t \in [i\,NT_r\ (i+1)NT_r] \tag{6b}$$

That is, the working point stays NT_r seconds in each occupied position. As $w(s)=G(s)u(s)$ and $G(s)$ is asymptotically stable, it follows from (6a-b) that:

$$\lim_{N\rightarrow\infty} w((i+1)NT_r) \in \{f_d(v_m), f_a(V_{i+1})\} \tag{7a}$$

using the fact that $G(0)=1$. On the other hand, one has from (1):

$$\lim_{N\rightarrow\infty} \frac{1}{NT_r}\int_{iNT_r}^{(i+1)NT_r} y(t) = \lim_{N\rightarrow\infty} \frac{1}{NT_r}\int_{iNT_r}^{(i+1)NT_r} w(t) \tag{7b}$$

using the fact that the white noise ξ in (1) is ergodic and zero-mean. Combining (7a-b) one gets:

$$\left(\lim_{N\rightarrow\infty} \frac{1}{NT_r}\int_{iNT_r}^{(i+1)NT_r} y(t)\right) \in \{f_d(v_m), f_a(V_{i+1})\}$$

which, together with (5) implies that:

$$\lim_{N\rightarrow\infty} \hat{W}_{i+1}(N) \in \{f_d(v_m), f_a(V_{i+1})\},\quad i=0\ldots n-1 \tag{8}$$

Combining (6a-b) and (8) it follows that, for $i=0\ldots n-1$:

$$\lim_{N\rightarrow\infty}\left(V_{i+1},\ \hat{W}_{i+1}(N)\right) \in \{(V_{i+1}, f_d(v_m)), (V_{i+1}, f_a(V_{i+1}))\} \subset \mathcal{P}_a$$

which proves the first part of Proposition 1. The second part is similarly established ■

IV. Linear Subsystem Identification

In this section, an identification method is proposed to get estimates of the linear subsystem complex gain $G(jk\omega)$ at the frequencies $k\omega$ $(k=0,1,2\ldots)$, whatever $\omega>0$. From the NBBI procedure (Table 1), one gets estimates of a set of $2n-2$ different points of the backlash limit cycle $\mathcal{C} \overset{def}{=} \mathcal{P}_a \cup \mathcal{P}_d$. Furthermore, the larger the parameter N is, the better the estimation accuracy. For simplicity, we presently suppose that the estimated points have been exactly determined and, for clarity, the determined points are denoted:

$$(V_{i+1}, U_{i+1}),\ i=0\ldots 2n-3 \tag{9}$$

To get profit from this result, the system is excited by a periodic input signal $v(t)$, with period $T = 2\pi/\omega$, that only takes the values V_i:

$$v(t) \in \{V_i; i = 1 \ldots 2n-2\} \tag{10}$$

Furthermore, the above values come in the same order as in (4a), i.e. $V_1 \to V_2 \to V_3 \ldots \to V_{2n-3}$, and each one is kept on during $T/(2n-2)$ seconds. Doing so, it is clear from Fig. 5 that, if the backlash working point (v,u) occupies initially position ① then, $(v(t),u(t))$ will stay all time on the limit cycle $\mathcal{C} \overset{def}{=} \mathcal{P}_a \cup \mathcal{P}_d$ occupying there only the positions (V_i,U_i), $i = 1 \ldots 2n-2$, defined in (9). Then, the backlash output $u(t)$ turns out to be perfectly known. Specifically, $u(t)$ is in turn periodic, with period T, and

$$u(t) \in \{U_i; i = 1 \ldots 2n-2\} \tag{11}$$

Furthermore, the above values of $u(t)$ come in the order $U_1 \to U_2 \to U_3 \ldots \to U_{2n-3}$. Since $u(t)$ is periodic and known, it can be developed in Fourier series:

$$u(t) = \frac{a_0}{2} + \sum_{k=1}^{\infty} a_k \cos(k\omega t) + b_k \sin(k\omega t) \tag{12}$$

with:

$$a_k = \frac{2}{T}\int_0^T u(t)\cos(k\omega t)dt\,,\; b_k = \frac{2}{T}\int_0^T u(t)\sin(k\omega t)dt \tag{13}$$

where $k = 0,1,2\ldots$. As $G(s)$ is asymptotically stable and $G(0) = 1$, it follows from (12) that the steady state undisturbed output (given that $w(s) = G(s)u(s)$) is of the form:

$$w(t) = \frac{a_0}{2} + \sum_{k=1}^{\infty} a_k \left|G(jk\omega)\right| \cos(k\omega t + \angle G(jk\omega)) + \sum_{k=1}^{\infty} b_k \left|G(jk\omega t)\right| \sin(k\omega t + \angle G(jk\omega)) \tag{14}$$

As $y(t) = w(t) + \xi(t)$, one immediately gets from (14):

$$y(t) = \frac{a_0}{2} + \sum_{k=1}^{\infty} a_k \left|G(jk\omega)\right| \cos(k\omega t + \angle G(jk\omega)) + \sum_{k=1}^{\infty} b_k \left|G(jk\omega)\right| \sin(k\omega t + \angle G(jk\omega)) + \xi(t) \tag{15}$$

Using standard trigonometric formulas, the right side of (15) simplifies to:

$$y(t) = \frac{a_0}{2} + \sum_{k=1}^{\infty} \alpha_k \cos(k\omega t) + \beta_k \sin(k\omega t) + \xi(t) \tag{16}$$

with:

$$\alpha_k = \left|G(jk\omega)\right|\left(a_k \cos(\angle G(jk\omega)) + b_k \sin(\angle G(jk\omega))\right) \tag{17a}$$

$$\beta_k = \left|G(jk\omega)\right|\left(b_k \cos(\angle G(jk\omega)) - a_k \sin(G(jk\omega))\right) \tag{17b}$$

Squaring both sides of (17a-b) and combining the resulting equalities one gets:

$$\left|G(jk\omega)\right| = \frac{\sqrt{\alpha_k^2 + \beta_k^2}}{\sqrt{a_k^2 + b_k^2}} \tag{18}$$

Also, solving (17a-b) for $\cos(\angle G(jk\omega))$ and $\sin(\angle G(jk\omega))$ yields:

$$\cos(\angle G(jk\omega)) = \frac{a_k\alpha_k + b_k\beta_k}{\sqrt{a_k^2 + b_k^2}\sqrt{\alpha_k^2 + \beta_k^2}} \tag{19a}$$

$$\sin(\angle G(jk\omega)) = \frac{b_k\alpha_k - a_k\beta_k}{\sqrt{a_k^2 + b_k^2}\sqrt{\alpha_k^2 + \beta_k^2}} \tag{19b}$$

Equations (18)-(19a-b) show how to obtain the complex amplitudes $G(jk\omega)$ $(k = 1,2\ldots)$ using the two couples (a_k,b_k) and (α_k,β_k). As the first is already available by (13), it remains to estimate the second. This is performed noticing that the right side of (16) is nothing other than the Fourier series expansion of the output signal $y(t)$, up to noise ξ. Given that all deterministic terms on the right side of (16) are periodic, with common period T, and ξ is a zero-mean ergodic white noise, the effect of the latter can be filtered considering the following trans-period averaging of the output:

$$y_f(t,M) = \frac{1}{M}\sum_{i=1}^{M} y(t + (i-1)T)\,, \quad 0 \le t < T \tag{20}$$

for some (large enough) integer M. Indeed, it is readily obtained using (16) and (20):

$$\lim_{M\to\infty} y_f(t,M) = \frac{a_0}{2} + \sum_{k=1}^{\infty} \alpha_k \cos(k\omega t) + \beta_k \sin(k\omega t) + \frac{1}{M}\sum_{i=1}^{M} \xi(t + (i-1)T) = \frac{a_0}{2} + \sum_{k=1}^{\infty} \alpha_k \cos(k\omega t) + \beta_k \sin(k\omega t) \tag{21}$$

where the last equality holds with probability 1 because ξ is ergodic and zero-mean[1]. That is, the α_k's and β_k's turns out to be (w.p.1) the limits of Fourier series coefficients of $y_f(t,M)$ as $M \to \infty$. The latter are given by:

$$\alpha_k(M) = \frac{2}{T}\int_0^T y_f(t,M)\cos(k\omega t)dt\,, (k = 1,2,3\ldots) \tag{22a}$$

$$\beta_k(M) = \frac{2}{T}\int_0^T y_f(t,M)\sin(k\omega t)dt \tag{22b}$$

[1] By ergodicity, the (common) mathematic mean of the random variables $\xi(t + (i-1)T)$ coincides, with probability 1, with the arithmetic mean of any realization of the random variable sequence $\{\xi(t + (i-1)T), i = 1,2,3\ldots\}$ (for any fixed $t \in [0\ T)$).

Then, it follows from (21) that:

$$\lim_{M\to\infty}\alpha_k(M)=\alpha_k \quad \text{and} \quad \lim_{M\to\infty}\beta_k(M)=\beta_k \quad \text{(w.p.1)} \qquad (23)$$

The above results are based upon to get estimates $\hat{G}_M(jk\omega)$ of the complex amplitudes $G(jk\omega)$ $(k=1,2\ldots)$, for any fixed $\omega>0$. This is performed using the identification procedure of Table 2.

Table 2. Frequency Gain Identification (FGI)

1. Initialization experiment

Similar to Table 1 (Step 1).

2. Data acquisition

- Choose a frequency ω, let $T=2\pi/\omega$ and $\tau=T/(2n-2)$.
- Apply the periodic signal, with period T, defined on the period $[0\ T)$ as follows:

$$v(t)=V_i \ \text{ for } \ t\in\left[(i-1)\tau\ \ i\tau\right),\ i=1,\ldots 2n-2 \qquad (24)$$

- Take a sufficiently long record of the resulting steady state output signal. Let this be denoted $y(t)$, $t\in[0\ M\ T]$ for some integer $M>>1$.

3. Data processing

- From the input sequence $v(t)$, generate the corresponding output backlash signal $u(t)$, using the expressions (9) to (11) and accompanying remarks, and compute its Fourier series coefficients a_k and b_k using (13).
- Generate the filtered output $y_f(t,M)$ using (20) and compute its Fourier series coefficients $\alpha_k(M)$ and $\beta_k(M)$ using (22a-b).
- Compute the estimates $\hat{G}_M(jk\omega)$ using (18)-(19a-b) replacing there α_k and β_k by $\alpha_k(M)$ and $\beta_k(M)$, respectively, i.e.

$$\left|\hat{G}_M(jk\omega)\right|=\frac{\sqrt{\alpha_k^2(M)+\beta_k^2(M)}}{\sqrt{a_k^2+b_k^2}} \qquad (25)$$

$$\cos(\angle\hat{G}_M(jk\omega))=\frac{a_k\alpha_k(M)+b_k\beta_k(M)}{\sqrt{a_k^2+b_k^2}\sqrt{\alpha_k^2(M)+\beta_k^2(M)}} \qquad (26a)$$

$$\sin(\angle\hat{G}_M(jk\omega))=\frac{b_k\alpha_k(M)-a_k\beta_k(M)}{\sqrt{a_k^2+b_k^2}\sqrt{\alpha_k^2(M)+\beta_k^2(M)}} \qquad (26b)$$

Proposition 2. The estimates $\hat{G}_M(jk\omega)$ obtained by the FGI procedure (Table 2) are consistent estimates i.e. $\hat{G}_M(jk\omega)\to G(jk\omega)$ w.p. 1 as $M\to\infty$ □

Proof. Comparing (25)-(26a-b) to (18)-(19a-b), it is readily seen, using (23), that $\hat{G}_M(jk\omega)$ converges in probability to $G(jk\omega)$ ■

Remark 2.

a) The FGI procedure can be repeated as many times as wished considering each time a different value of the frequency ω.

b) For a given ω, the number of estimates $\hat{G}_M(jk\omega)$ $(k=1,2,3\ldots)$ to be determined may be arbitrarily large. Practically, it is reasonable to limit the number of estimates to those frequencies for which the Fourier series coefficients (a_k, b_k) of $u(t)$ are significant. According to the Parseval's identity one has (e.g. [5]):

$$\frac{a_0^2}{4}+\sum_{k=1}^{\infty}\frac{a_k^2+b_k^2}{2}=\frac{1}{T}\int_0^T u^2(t)dt<\infty \qquad (27)$$

where the right side of the equality represents the power of the signal $u(t)$. It readily follows from (27) that $\sum_{k=p}^{\infty}\frac{a_k^2+b_k^2}{2}\to 0$ as $p\to\infty$. Then, it is reasonable to consider as significant only the coefficient list $(a_k, b_k;\ k=1\ldots p)$ where p is such that:

$$\frac{a_0^2}{4}+\sum_{k=1}^{p}\frac{a_k^2+b_k^2}{2}\geq(1-\varepsilon)\frac{1}{T}\int_0^T u^2(t)dt$$

for some $0<\varepsilon<<1$ chosen by the user.

c) Finally, note that the frequencies, $k\omega\,(k=1,2,3\ldots)$, for which the complex amplitudes $G(jk\omega)$ are estimated in the FGI procedure, are independent on the number and positions of the points, (V_i,U_i) $(i=1\ldots 2n-2)$, estimated in the NBBI procedure. In fact, ω is only imposed by the user through the choice of the period T of the excitation signal $v(t)$ defined by (24). Accordingly, the latter needs not to take all values, V_i $(i=1\ldots 2n-2)$, involved in the NBBI procedure □

REFERENCES

[1] E.W. Bai.(2002). 'Identification of linear systems with hard input nonlinearities of known structure'. Automatica , vol 38, pp. 853-860.

[2] F. Giri, Y. Rochdi, F.Z. Chaoui, A. Brouri. (2008). 'Identification of Hammerstein systems in presence of hysteresis-backlash and hysteresis-relay nonlinearities'. Automatica, vol. 44, pp 767-775

[3] Cerone, V, & Regruto, D. (2007). 'Bounding the parameters of linear systems with input backlash'. IEEE Transactions on Automatic Control, 52, 531_536.

[4] Y. Rochdi, F. Giri, B. Gning, F.Z. Chaoui, (2010). 'Identification of block-oriented systems in presence of nonparametric input nonlinearities of switch and backlash types'. Automatica, vol. 46, pp. 864-877.

[5] L. Ljung, 'System Identification - Theory for the User', Prentice-Hall, Englewood Cliffs, N J, 1987.